Journal of Applied Physics ARTICLE pubs.aip.org/aip/jap

Statistical analysis of displacement damage in small devices from neutron and ion irradiation

Cite as: J. Appl. Phys. **136**, 204501 (2024); doi: 10.1063/5.0237175
Submitted: 3 September 2024 · Accepted: 7 November 2024 ·
Published Online: 25 November 2024

W. R. Wampler,[a] G. Vizkelethy, and M. Titze

AFFILIATIONS

Sandia National Laboratories, Albuquerque, New Mexico 87111-1056, USA

[a]**Author to whom correspondence should be addressed:** wrwampl@sandia.gov

ABSTRACT

Modern semiconductor devices, such as gate-all-around nanosheet field-effect transistors (GAA NS FETs), are smaller than displacement damage cascades from fission neutrons. In this regime, device failure may occur through low-probability single events, rather than by parametric degradation previously seen in larger devices. Here, we present a statistical model that predicts the probability of a damage event in a small device and the probability distribution of the magnitude, i.e., number of displacements within the device, from each event. The model is developed first for neutron irradiation and then for energetic ion irradiation. The model is consistent with results from recent experiments in which lithium-ion irradiation produced stepwise increases in subthreshold current in GAA NS FETs.

I. INTRODUCTION

Displacement damage from energetic particle irradiation degrades the operation of electronic devices such as transistors. Metal–oxide–semiconductor (MOS) technologies tend to be less sensitive to displacement damage than junction transistors because they are majority carrier devices but are still degraded by sufficiently high damage levels. State-of-the-art semiconductor technology is now using gate-all-around nano-sheet field-effect transistors (GAA NS FETs),[1,2] which are much smaller than previous finFET and planar CMOS technologies. Displacement damage in these very small devices is different from earlier larger devices. Devices are now smaller than displacement damage cascades from fission neutrons. In this regime, damage in a device must be characterized by the probability of an event producing atomic displacements within the device, and the probability distribution of the magnitude, i.e., number of displacements, of each event, rather than by a parametric degradation with average damage per unit volume. For neutron fluences of practical interest, the separation between displacement cascades is large compared to the spatial extent of individual cascades, but the density of defects within cascades is high. Hence, the probability that an individual transistor will be damaged is very small, but the defect concentration within a device that is struck, and, hence the impact on its operation, may be large. The low probability of a damage event makes tests of effects from neutron irradiation difficult. Such tests must be done either on a very large number of devices or alternatively with impractically high neutron fluences to insure a damage event in a single device. Consequently, tests are being conducted in which displacement damage is produced by ion-irradiation.[3] In these tests, stepwise increases in subthreshold leakage current were observed in GAA NS FET devices from individual ion strikes, and higher damage levels permanently turned off forward current.

Here, we describe a new analytical method to characterize displacement damage in small devices, which can be used to relate effects seen in ion-irradiation tests, to those predicted to occur from neutron irradiation. The model enables the predictions of how the damage varies with irradiation conditions, such as device geometry size and composition, fluence and energy spectrum of neutrons, or type fluence, and energy of ions.

Quantitative modeling of the influence of lattice defects on device operation is beyond the scope of this study. Here, we focus on the probability that a device will be damaged and amount of damage expected in a small device. The methodology described here predicts the probability and amount of displacement damage from neutron and ion irradiation in devices smaller than the damage cascades, which enables the prediction of how failure rates might change as technology evolves to smaller devices.

The literature on radiation effects in materials and electronic devices is vast. A general overview with many references can be found in Ref. 4. A related previous study[5] examined the distribution of non-ionizing energy loss in small volume elements representing image sensors with dimensions of the order 1–10 μm. Here, we examine defect production in much smaller volume elements representing GAA NS FET devices.

II. METHOD

The method is based on simulations of displacement cascades using Marlowe[6] or SRIM[7] binary collision codes. These simulations give the spatial coordinates of each defect in each cascade. Here, we use vacancies to represent the displacement damage. A statistical analysis is done on the spatial distribution of vacancies produced, to determine the probability of a damage event occurring in a device and the probability distribution of the amount of damage per event. The model approximates the device as a small volume element (voxel) embedded within the bulk material to represent the sensitive region of the device, such as the channel of a GAA NS. We illustrate the method for the case of silicon devices.

The use of the binary collision approximation (BCA) to calculate displacement damage is justified by a comparison[8] of defect production from simulations using the BCA code Marlowe[6] and the molecular dynamics code Large-scale Atomic/Molecular, Massively Parallel Simulator (LAMMPS).[9,10] Molecular dynamics (MD) codes are expected to be more accurate at low collision energies. In MD simulations, collisions at energies below a certain threshold do not produce stable interstitial-vacancy pairs. This effect can be included in Marlowe simulations through a cut-off separation below which the defects are dynamically unstable against prompt recombination and are not counted. A cut-off distance of 7.4 ± 0.09 Å gives very close agreement between Marlowe and LAMMPS for defect production in silicon. The SRIM BCA code uses a displacement threshold energy to cut off defect production at low recoil energies. However, this displacement threshold energy is not a well-defined parameter. For example, it depends on the angle of the recoil with respect to the crystal lattice. The effect of the displacement threshold energy in SRIM is similar to the cut-off distance used in Marlowe; a smaller displacement threshold gives more defects. Consequently, here we use a value for the displacement threshold energy in SRIM, which gives the same defect production as Marlowe and LAMMPS. This value is 21 eV, which is within the range of values determined experimentally.

BCA codes give the initial defect distribution before any evolution due to thermally activated migration and reaction of defects. The annealing of displacement damage is known to occur in silicon at room temperature,[11] but quantitative atomistic treatment is complex[12] and goes beyond the scope of this work.

A. Neutrons

For neutron irradiation, the primary recoil energies were randomly sampled from distributions calculated from the EMPIRE neutron scattering code[13] using scattering cross sections from the ENDF database,[14] for various neutron energy distributions. Figure 1 shows the distribution of recoil energies in silicon for fission neutron spectra from the Annular Core Research Reactor at Sandia National Laboratories[15] and for monoenergetic 14 MeV neutrons from deuterium–tritium fusion.

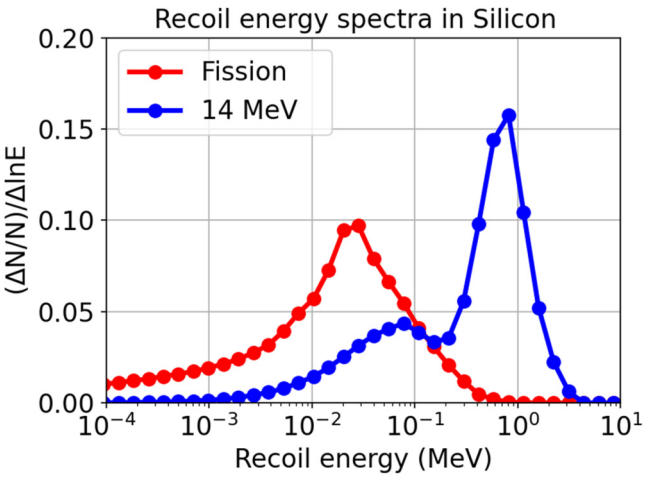

FIG. 1. Probability distribution of the recoil energy in silicon from fission and fusion neutrons.

Figure 2 shows an example of the recoil cascades produced by fission neutrons. The defect maps are subdivided into a grid of small volume elements or voxels, and the distribution $f(N_V)$ of the

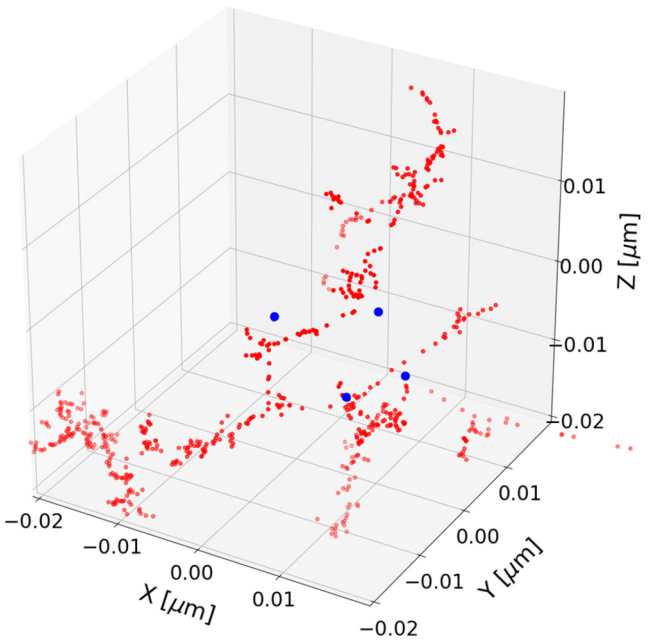

FIG. 2. Marlowe simulations of cascades from four primary collisions with recoil energies between 9 and 41 keV, showing the location of primary collision (blue dots), and individual vacancies (red dots) within cascades.

number of voxels containing N_V vacancies per cascade is calculated, averaged over many cascades. The average number of voxels per collision that have damage, i.e., have $N_V > 0$, is $N_{vxl} = \sum f(N_V)$, so that the normalized probability that a voxel has N_V vacancies given that $N_V > 0$ is

$$f_n(N_V) = f(N_V)/N_{vxl}. \quad (1)$$

Figure 3 shows the normalized probability distribution of the number of vacancies within a voxel per collision $f_n(N_V)$, i.e., the fraction of damaged voxels that have N_V vacancies, for fission and 14 MeV neutrons on silicon and for various device sizes. Damage events from 14 MeV neutrons are more likely to have a small number of vacancies and less likely to have a large number of vacancies than fission neutrons. This is due to the higher recoil energies from 14 MeV neutrons (see Table I). The variation in damage with neutron energy is not large. For both neutron spectra, most damage events have only a small number of vacancies, but a small fraction have up to a few hundred vacancies within the voxel. Smaller voxels are more likely to have a smaller number of vacancies and less likely to have a large number of vacancies.

Next, consider the probability λ that a voxel has been damaged, i.e., has $N_V > 0$. This is given by N_{vxl} the number of voxels per collision with $N_V > 0$ times the number of collisions per unit volume $\alpha\phi$ divided by the total number of voxels per unit volume $(1/V)$, where V is the volume of one voxel,

$$\lambda = \alpha\varphi\, N_{vxl}\, V. \quad (2)$$

where ϕ is the neutron fluence and α is the number of collisions per unit volume per unit neutron fluence (see Table I). The

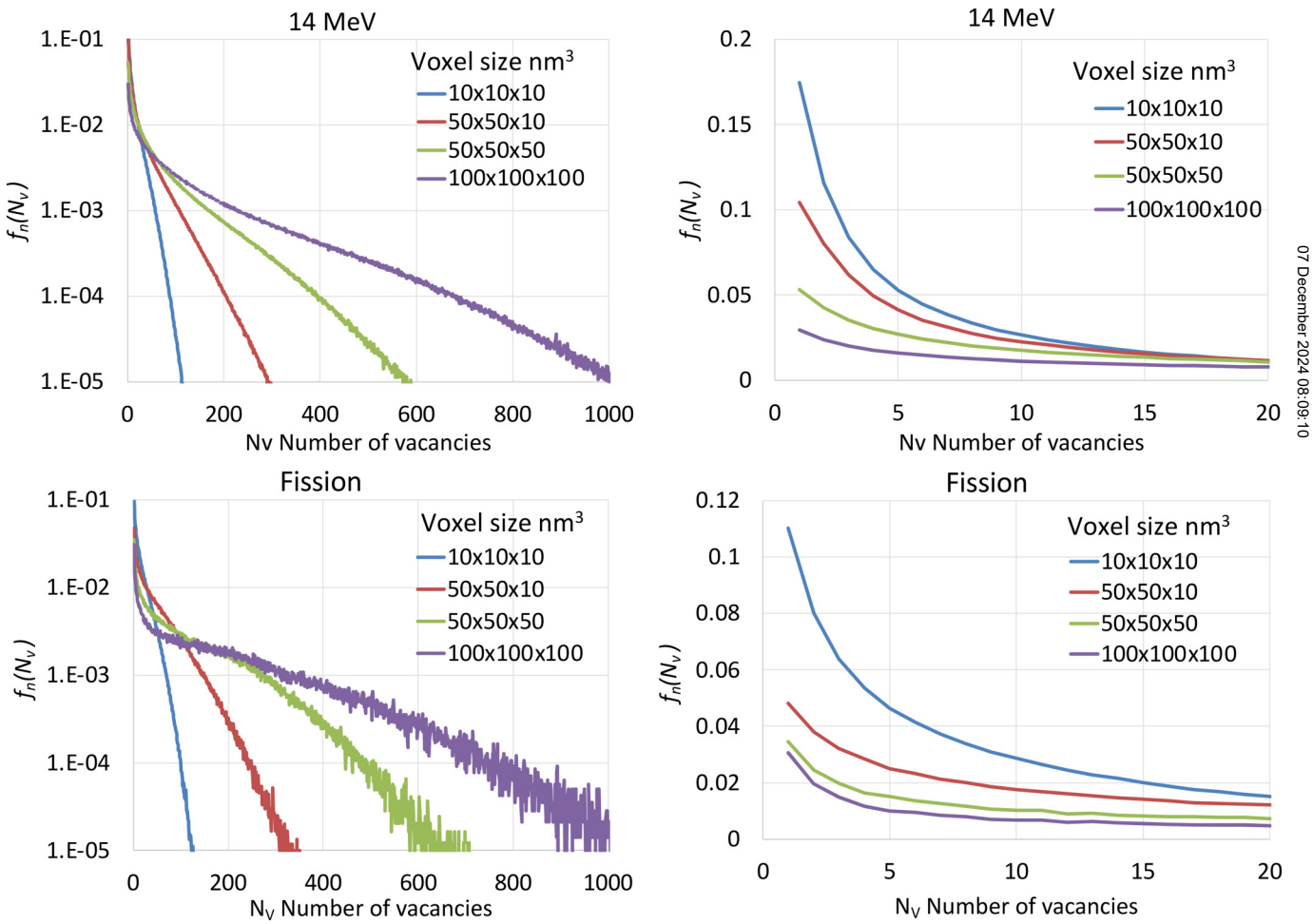

FIG. 3. Normalized probability distribution of the number of voxels with N_V vacancies per cascade for 14 MeV neutrons (above) and fission neutrons from ACRR (below) in silicon for various voxel sizes with logarithmic (left) and linear (right) vertical scales to more clearly show differences at both large (left) and small (right) number of vacancies.

TABLE I. Collision rate coefficient, mean recoil energy, and mean number of vacancies per collision from Marlowe, for fission and fusion neutrons in silicon.

	α (collisions/cm^3)/ (neutron/cm^2)	Recoil energy (keV)	Defects/collision (Marlowe)
Fission	0.151	40	269
14 MeV	0.091	570	1510

probability $P(N_V)$ that a device, represented by a voxel, has N_V vacancies is, therefore, the probability λ that it has been damaged (i.e., has $N_V > 0$) times the probability of having N_V vacancies given that $N_V > 0$,

$$P(N_V) = f_n(N_V)\,\lambda = \frac{f(N_V)}{N_{vxl}}\alpha\varphi\, N_{vxl}\, V = f(N_V)\,\alpha\varphi V. \quad (3)$$

This is a compound Poisson process,[16] with average number or rate of events λ and normalized probability distribution $f_n(N_V)$ for the magnitude (here the number of vacancies N_V) of each event.

Larger devices have a higher probability of having more defects but also contain more silicon atoms. As a metric relating damage to its influence on device operation and the probability of failure, we use the vacancy concentration within a voxel, i.e., the number of vacancies per silicon atom within the device $C_V = N_V/N_{Si}$. Furthermore, we argue that if N_V vacancies cause a device to fail, then it should also fail if it has more than N_V vacancies; hence, the probability of failure should be related to the cumulative probability that the vacancy concentration within the device exceeds a specified value. The probability distribution of this quantity is plotted in Fig. 4 for various device sizes and for a fluence of 10^{13}/cm^2 14 MeV neutrons. This is a quantity that should be related to the frequency or probability of device failure observed in tests. According to this analysis, the likelihood of having a high vacancy concentration is much larger in smaller devices. Table II shows that as the voxel size decreases, the probability λ that a voxel will be damaged decreases, but the average vacancy concentration in voxels that are damaged increases.

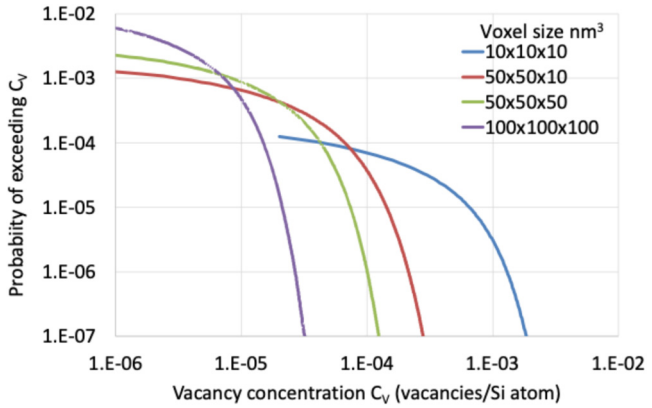

FIG. 4. Probability that the vacancy concentration in a voxel will exceed the value C_V for various voxel sizes and for a fluence of 1×10^{13}/cm^2 of 14 MeV neutrons.

B. Ions

Damage in small devices by ion irradiation can be quantified using a method analogous to that described above for neutrons. Neutrons produce damage from primary recoils at random locations throughout the volume, whereas ions enter the material at a surface and produce displacement damage along tracks within their range, which depends on the type and energy of ion and type of the material. Here, we illustrate the method for a configuration approximating that of recent tests[3] in which a GAA NS FET was irradiated with 35 keV lithium ions. In those tests, the subthreshold leakage current exhibited stepwise increases, which were ascribed to single ion strikes, possibly with only a few, or a single atomic displacement within a device. Such measurements, along with simulations of damage described here, reveal the influence of displacement damage on GAA NS FET operation. Effects of ion irradiation on device operation can then be used to predict the effects from neutron irradiation using the model described here. In the Li ion irradiation tests, the dimensions of the region of the device sensitive to damage, assumed to be the channel, were of the order 5 nm thick and 50 × 50 nm wide.[2] As with neutron damage, the model for ion damage uses a simplifying approximation that the device is a region with specified thickness and lateral dimensions within a silicon matrix.

Displacement damage from ions was simulated using the binary collision particle transport code SRIM in full cascade mode with a displacement threshold energy of 21 eV chosen to match defect production in Marlowe simulations. Figure 5 shows C_v the vacancy concentration per unit ion fluence vs depth for 35 keV lithium ions on silicon. The average number of vacancies produced per ion is $\int C_V dx = 212$.

From Fig. 5, the average number of vacancies produced per ion is $\langle N_V \rangle = C_V\, dx = 3.5$ vac/ion for devices of thickness $dx = 5$ nm at a depth $x = 250$ nm beneath the surface, for example, due to an overlying planarization layer.

However, there is a large variation in the number of vacancies per ion within dx. Some ions never reach dx, some pass through dx without making vacancies, and some produce energetic recoil cascades with many vacancies within dx, for example, as depicted in Fig. 6.

The defect coordinate files are processed to obtain

(a) α, the fraction of ions producing vacancies in a layer of thickness dx at depth x
(b) $f_n(N_V)$, the normalized probability distribution of N_V the number of vacancies within dx per damage event, i.e., for ions with $N_V > 0$.

For example, with $dx = 5$ nm at a depth $x = 250$ nm, the fraction of ions producing a damage event within dx, i.e., the mean number of damage events within dx per incident ion is $\alpha = 0.35$.

TABLE II. Average number of damaged voxels (i.e., with $N_V > 0$) per collision N_{vxl} and λ the probability a voxel (i.e., device) will be damaged, i.e., has $N_V > 0$, for a neutron fluence $\phi = 10^{13}/\text{cm}^2$, and mean number of vacancies per silicon atom in damaged voxels, for fission and fusion neutrons in silicon and for three device sizes.

	$10 \times 10 \times 10$ nm			$50 \times 50 \times 10$ nm			$100 \times 100 \times 100$ nm		
	N_{vxl}	λ	$\langle N_V \rangle$ vac/N_{Si}	N_{vxl}	λ	$\langle N_V \rangle$ vac/N_{Si}	N_{vxl}	λ	$\langle N_V \rangle$ vac/N_{Si}
Fission	17.2	2.60×10^{-5}	3.1×10^{-4}	6.0	2.28×10^{-4}	3.6×10^{-5}	1.4	2.16×10^{-3}	3.18×10^{-6}
14 MeV	137.5	1.25×10^{-4}	2.2×10^{-4}	58.0	1.32×10^{-3}	2.1×10^{-5}	11.6	1.05×10^{-2}	2.6×10^{-6}

The normalized probability distribution of the number of vacancies per event $f_n(N_V)$ is shown in Fig. 7.

The probability a damage event has a single vacancy is 0.19. The mean number of vacancies in dx per incident ion is 5.6, and the mean number of vacancies per damage event within dx is

$$\sum_{N_V} N_V \, f_n(N_V) = 10.3.$$

With an ion fluence φ, the probability of an event occurring, which has N_V vacancies in a device of lateral area A, is

$$P(N_V) = f_n(N_V)\, \lambda, \tag{4}$$

where $\lambda = \alpha \varphi \, A$ is the probability of a damage event within area A and $f_n(N_V)$ is the fraction of events that have N_V vacancies within dx.

For device lateral area $A = 50 \times 50 = 2500\ \text{nm}^2$, the ion fluence to see an average of one event (i.e., $\lambda = 1$) is $\varphi = 1/(\alpha\, A) = 1.1 \times 10^{11}$ ions/cm^2.

The above analysis assumes that the N_V vacancies in the layer from individual ions are all within a single device of area A. Allowing for ions that produce damage in multiple adjacent devices, the damage can be analyzed as follows. Divide the layer with thickness dx at depth x into a 2D grid of pixels of lateral dimensions dy,dz. Evaluate α the fraction of ions that make vacancies in dx. For ions producing damage in dx, count $N_p(N_V)$ the number of pixels that have N_V vacancies per event, and $N_{pav} = \sum N_p(N_V)$, the average number of damaged pixels per damage event.

The normalized probability that a damage event in a pixel has N_V vacancies is

$$p(N_V) = \frac{N_p(N_V)}{N_{pav}}, \tag{5}$$

For an ion fluence φ, the probability that a particular pixel (i.e., device) has N_V vacancies is given by

$$P_p(N_V) = p(N_V)\, \lambda, \tag{6}$$

where

$$\lambda = N_{pav}\, \alpha\, \varphi\, A \tag{7}$$

is the probability of a damage event in a pixel.

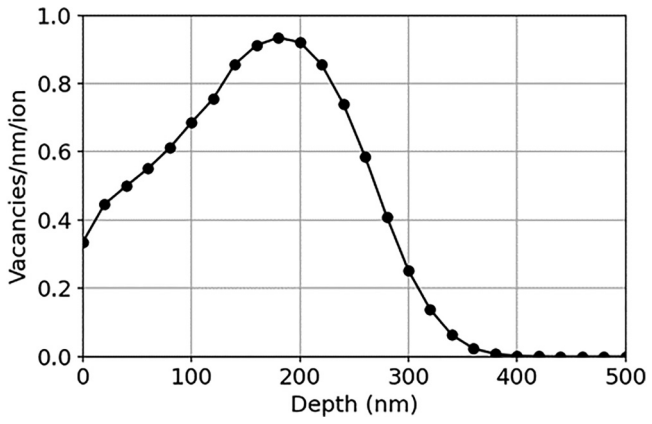

FIG. 5. Vacancy concentration per unit ion fluence from Marlowe for 35 keV Li ions on silicon.

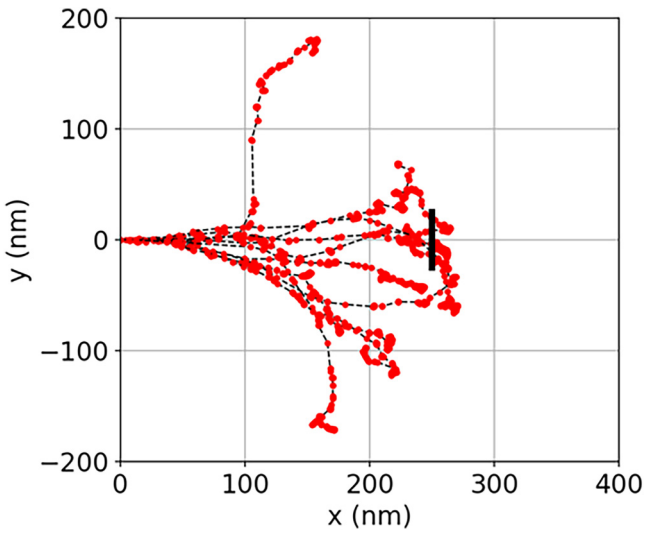

FIG. 6. Spatial distribution of vacancies (red dots) from ten ions projected onto the xy plane from a SRIM simulation. 35 keV Li ions at normal incidence at x, $y = 0,0$. The bar represents a device $dx = 5$ nm thick and $dy = 50$ nm wide at depth $x = 250$ nm.

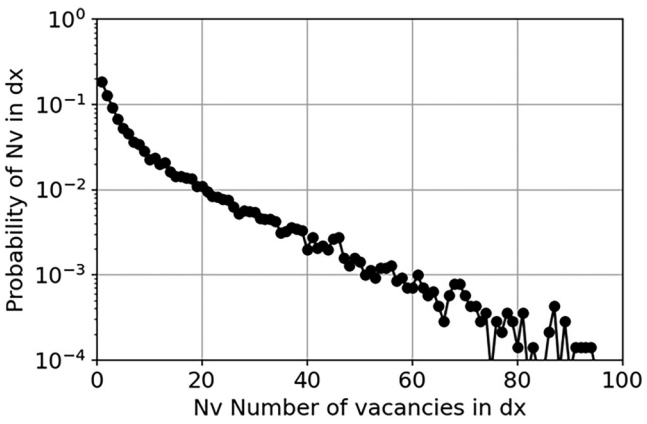

FIG. 7. Normalized probability distribution of a damage event within *dx* having N_V vacancies.

Equations (5)–(7) for a 2D grid of area elements (pixels) are analogous to Eqs. (1)–(3) for a 3D grid of volume elements (voxels).

For 35 keV Li ions and an array of adjacent devices of thickness 5 nm and area 50 × 50 nm at a depth of 250 nm, the average number of devices damaged per ion making damage in *dx* is 1.24, i.e., most damage events damage only one device for devices of this size. Figure 8 (black curve) shows the probability distribution function p(N_V) for the number of vacancies per damage event in a pixel given by Eq. (4). The mean number of vacancies in a pixel per damage event for 35 keV Li ions is

$$\langle N_v \rangle = \sum_{N_V} N_V \, p(N_V) = 8.4,$$

and the fraction of events that produce a single vacancy is 0.20. Comparing Fig. 8 for ions to Fig. 4 for neutrons, 35 keV Li ions are more likely to produce damage events with a single vacancy and less likely to produce damage events with many (more than 20) vacancies. Variations in the probability distribution function of damage from ions with device size are similar to that shown in Fig. 3 for damage from neutrons, although with ions, the device thickness has a stronger effect than the lateral dimensions.

The model can also be used to predict damage for other experimental conditions. For example, Fig. 3 shows the dependence on the neutron energy spectrum and device size. Simulations for various ion types (Fig. 8) show that heavier ions produce more events with many vacancies and fewer events with small numbers of vacancies. This is due to the higher recoil energies with heavier ions. The vacancy probability distribution for heavier ions more closely resembles that of fission neutrons shown in Fig. 3. In addition, simulations have been done for different ion energies and device depth and size, and for materials other than silicon, such as SiGe alloys used in p-channel GAA NS FETs.

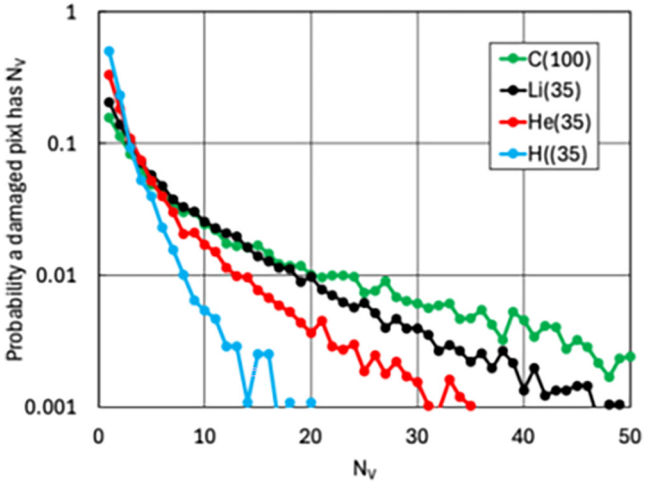

FIG. 8. Probability distribution for the number of vacancies *Nv* in damaged pixels for various ion types with energies (keV indicated in the legend) to approximately match depths of damage, and for a device with 5 nm thickness and 50 × 50 nm lateral dimensions at a depth of 250 nm.

III. EXPERIMENT

Previous studies have reported single-event displacement damage effects from ion-irradiation in semiconductor devices.[17–20] Here, we compare our model to recent tests in which displacement damage was produced in GAA NS FETs by ion-irradiation.[3] In these tests, stepwise increases in the sub-threshold leakage current were observed from individual ion strikes. GAA NS FET devices were irradiated with 35 keV lithium ions at the Sandia Ion Beam Laboratory. Experimental details and examples of the resulting changes in current are given in Ref. 3. Here, we compare two features of the model with the results from this experiment, the frequency of damage events λ, and the magnitude of the observed changes in current, presumed to be related to the amount of damage per event.

Figure 9 shows the ion fluence where the first step change in the current occurred Fig. 9(a) and the relative magnitude of the change for six devices tested Fig. 9(b). The mean ion fluence to produce a step in current was 2.0×10^{11} ions/cm^2. Although the device dimensions and overlayer thickness were not well known, this ion fluence is consistent with a device area of $A = 30 \times 30$ nm (from mean number of damage events $\lambda = \alpha\varphi A = 1$ with a fraction of incident ions producing damage at the depth of the device $\alpha \sim 0.5$), i.e., consistent with the model described above and the expected geometry for the GAA NS FET tested. In addition, the variance in the ion fluence to produce a step was 2×10^{11} ions/cm^2, i.e., as large as the mean value, which is consistent with the expected Poisson distribution for ion fluence to produce one event. While the data are sparse, a t-test on the data shows the 95% confidence interval for the mean to be $2.0 \times 10^{11} \pm 1.6 \times 10^{11}$ ions/cm^2. Figure 9(b) shows the relative magnitude of the first step change in the sub-threshold current for the six devices tested. Five of the

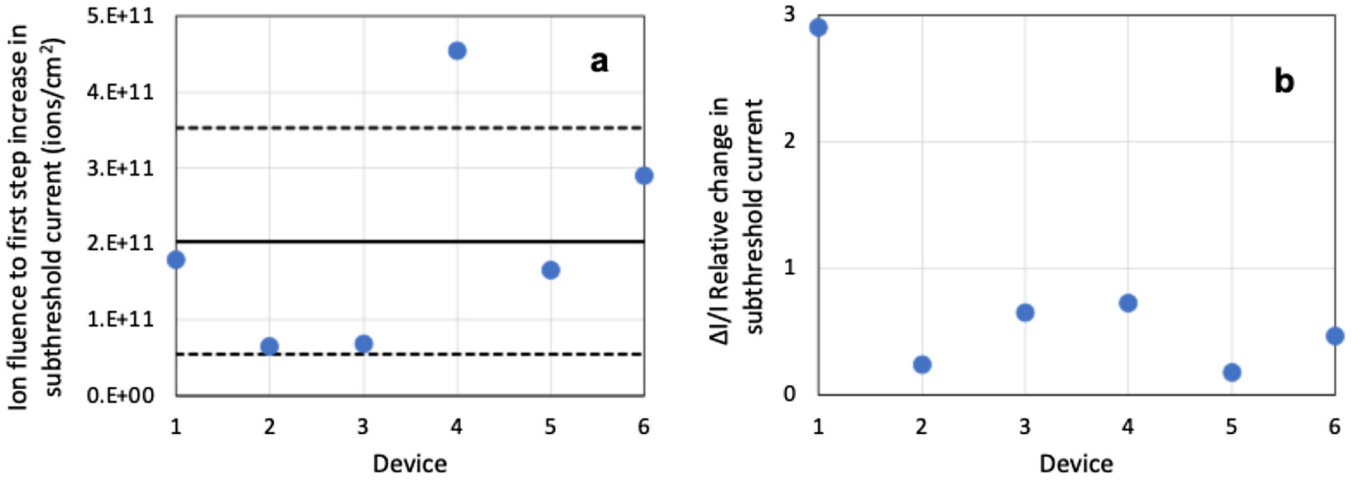

FIG. 9. (a) Ion fluence where the first step increase in the sub-threshold leakage current occurred in six devices tested. The horizontal solid line indicates the mean value, and the dashed lines show mean ± RMS variation. (b) Relative change in current in the first step.

devices had values from about 0.2 to 0.7 for the relative change in the current, but one had a larger increase of 2.9. If we assume that the magnitude of the relative current increase is proportional to the number of defects produced within the device channel, then these results are consistent with the model described above. As shown in Fig. 8, most of the damage events have a small number of vacancies. The variation in the current step size in devices 2–6 may reflect events with one to three vacancies, with a relative current increase per vacancy of about 0.25. The model also predicts that a small fraction of events will have a much larger number of vacancies, which is consistent with one device in six having a larger current step from a larger number of vacancies. A more statistically significant comparison between the model and experiment will come from a larger number of tests. The observed device response vs ion fluence is clearly correlated with the predicted number of defects produced. The actual defect configuration present at the time of the electrical measurement and potential effects of thermally activated defect migration and reaction, a.k.a. annealing, remain to be determined.

The experiments also show that a much higher ion fluence, i.e., many ion damage events in the device, is required to produce a large decrease in the drive current in the on condition [Fig. 6(b) in Ref. 3].

IV. CONCLUSIONS

A statistical model is presented for displacement damage in small devices from neutron or ion irradiation. The model gives the probability of a damage event occurring and the probability distribution of the amount of damage within the device per event. The influence of the device size and particle energy spectrum was examined. The likelihood of having a high defect concentration is much larger in smaller devices. The method is illustrated using conditions chosen to represent recent tests in which GAA NS FETs were damaged by lithium-ion irradiation.[3] Damage predicted by the model is consistent with the experimentally observed stepwise increases in the subthreshold leakage current from single ion collision events. Model predictions of damage distributions indicate that the observed effects may be caused by small numbers of defects, possibly single atomic displacements, since such events have higher probability. While the number of devices tested is small, the results so far are consistent with the statistical model for damage in small devices presented here.

The model predicts that most damage events produce a small number of defects within the device, but a small fraction of events produce many more defects. Ion irradiation experiments show that a small number of defects increase the subthreshold leakage current in a GAA NS FET but have little effect on the forward current. However, higher damage levels (roughly two orders of magnitude more corresponding to a concentration of order 10^{-4} defects/Si atom) cause a large reduction in the forward current. Hence, there is a small but finite probability that a single damage event will produce enough damage within a GAA NS FET to permanently turn off the forward current. Such low-probability events are difficult to observe experimentally in tests of single-device response to neutron irradiation but may be consequential for large scale integrated circuits with millions of devices. The probability that a single damage event will produce a high enough defect concentration to kill the device increases dramatically as devices become smaller.

ACKNOWLEDGMENTS

The neutron recoil energy spectra used here and shown in Fig. 1 were provided by Brian Hehr at Sandia National Laboratories. Sandia National Laboratories is a multi-mission laboratory managed and operated by National Technology & Engineering Solutions of Sandia, LLC (NTESS), a wholly owned subsidiary of Honeywell International Inc., for the U.S. Department of Energy's National Nuclear Security Administration (DOE/NNSA) under Contract No. DE-NA0003525. This written work

AUTHOR DECLARATIONS

Conflict of Interest

The authors have no conflicts to disclose.

Author Contributions

W. R. Wampler: Conceptualization (lead); Investigation (lead); Methodology (lead); Software (equal); Writing – original draft (lead); Writing – review & editing (lead). **G. Vizkelethy:** Investigation (equal); Methodology (equal); Software (equal). **M. Titze:** Investigation (equal); Validation (equal).

DATA AVAILABILITY

The data that supports the findings of this study are available within the article.

REFERENCES

[1]A. Elwailly, J. Saltin, M. J. Gadlage, and H. Y. Wong, "Radiation hardness study of L_G = 20 nm FinFET and nanowire SRAM through TCAD simulation," IEEE Trans. Electron Devices **68**(5), 2289–2294 (2021).
[2]M. Wang, "A review of reliability in gate-all-around nanosheet devices," Micromachines **15**, 269 (2024).
[3]M. Titze *et al.*, "Displacement damage, total ionizing dose, and transient ionization effects in gate-all-around field effect transistors," ACS Appl. Electron. Mater. **6**, 5759 (2024).
[4]A. Holmes-Seidel and L. Adams, *Handbook of Radiation Effects*, 2nd ed. (Oxford University Press, 2002).
[5]M. Raine, A. Jay, N. Richard, V. Goiffon, S. Girard, M. Gaillardin, and P. Paillet, "Simulation of single particle displacement damage in silicon—Part 1: Global approach and primary interaction simulation," IEEE Trans. Nucl. Sci. **64**, 133 (2017).
[6]T. Robinson and I. M. Torrens, "Computer simulation of atomic-displacement cascades in solids in the binary-collision approximation," Phys. Rev. B **9**(12), 5008–5024 (1974).
[7]J. F. Ziegler, M. D. Ziegler, and J. P. Biersack, "SRIM—The stopping and range of ions in matter (2010)," Nucl. Instrum. Methods Phys. Res., Sect. B **268**(11), 1818–1823 (2010).
[8]G. Vizkelethy and S. M. Foiles, "Determination of recombination radius in Si for binary collision approximation codes," Nucl. Instrum. Methods Phys. Res., Sect. B **371**, 111 (2016).
[9]J. S. Plimpton, see http://lammps.sandia.gov for *LAMMPS: Large-scale Atomic/Molecular, Massively Parallel Simulator*.
[10]J. S. Plimpton, "Fast parallel algorithms for short-range molecular dynamics," J. Comput. Phys. **117**, 1 (1995).
[11]H. H. Sander and B. L. Gregory, "Transient annealing in semiconductor devices following pulsed neutron irradiation," IEEE Trans. Nucl. Sci. **13**, 53 (1966).
[12]S. M. Myers, P. J. Cooper, and W. R. Wampler, "Model of defect reactions and the influence of clustering in pulse-neutron-irradiated Si," J. Appl. Phys. **104**, 044507 (2008).
[13]M. Herman, R. Capote, B. V. Carlson, P. Obložinský, M. Sin, A. Trkov, and V. Zerkin, "EMPIRE: Nuclear reaction model code system for data evaluation," Nucl. Data Sheets **108**, 2655 (2007).
[14]See http://www.nndc.bnl.gov/exfor/endf00.jsp for evaluated Nuclear Data File, Brookhaven National Nuclear Data Center.
[15]E. J. Parma, T. J. Quirk, L. L. Lippert, P. J. Griffin, G. E. Naranjo, and S. M. Luker, "Radiation characterization summary: ACRR 44-inch lead-boron bucket located in the central cavity on the 32-inch pedestal at the core centerline (ACRR-LB44-CC-32-cl)," Sandia Nat. Laboratories, Albuquerque, New Mexico, Technical Report, SAND2013–3406 (2013).
[16]S. M. Ross, *Introduction to Probability Models, Eighth Edition* (Academic Press, New York, 2003), p. 321.
[17]T. Shinada, T. Kurosawa, H. Nakayama, Y. Zhu, M. Hori, and I. Ohdomari, "A reliable method for the counting and control of single ions for single-dopant controlled devices," Nanotechnology **19**, 345202 (2008).
[18]G. Vizkelethy, E. S. Bielejec, and B. A. Aguirre, "Stochastic gain degradation in II-V heterojunction bipolar transistors due to single particle displacement damage," IEEE Trans. Nucl. Sci. **65**, 206 (2018).
[19]E. C. Auden, R. A. Weller, M. H. Mendenhall, R. A. Reed, R. D. Schrimpf, N. C. Hooten, and M. P. King, "Single particle displacement damage in silicon," IEEE Trans. Nucl. Sci. **59**, 3054 (2012).
[20]M. G. Esposito, J. E. Manuel, A. Privat, T. P. Xiao, D. Garland, E. Bielejec, and M. J. Marinella, "Investigating heavy-ion effects on 14-nm FinFETs process: Displacement damage versus total ionizing dose," IEEE Trans. Nucl. Sci. **68**, 724 (2021).